Supplement of Hydrol. Earth Syst. Sci., 30, 2493–2521, 2026
https://doi.org/10.5194/hess-30-2493-2026-supplement
© Author(s) 2026. CC BY 4.0 License.

Hydrology and Earth System Sciences
Open Access
EGU

Supplement of

What can hydrological modelling gain from spatially explicit parameterization and multi-gauge calibration?

Xudong Zheng et al.

Correspondence to: Dengfeng Liu (liudf@xaut.edu.cn)

The copyright of individual parts of the supplement might differ from the article licence.

Table S1. Pairwise t-test results of the ensemble performance metrics (KGE) for the top 40 ranked optimization results across all calibration cases. The table shows the t-statistics for the comparison between each pair of cases, with significant differences indicated by asterisks ($p < 0.05$).

	Case 1	Case 2	Case 3	Case 4	Case 5	Case 6	Case 7	Case 8
Case 1	–	7.357*	6.820*	-11.652*	0.512	11.331*	2.965*	7.056*
Case 2	-7.357*	–	5.431*	-12.681*	0.189	11.040*	-0.471	6.920*
Case 3	-6.820*	-5.431*	–	-13.425*	-1.082	9.668*	-5.316*	6.343*
Case 4	11.652*	12.681*	13.425*	–	3.842*	13.970*	12.084*	8.459*
Case 5	-0.512	-0.189	1.082	-3.842*	–	8.108*	-0.234	6.308*
Case 6	-11.331*	-11.040*	-9.668*	-13.970*	-8.108*	–	-11.050*	1.568
Case 7	-2.965*	0.471	5.316*	-12.084*	0.234	11.050*	–	6.935*
Case 8	-7.056*	-6.920*	-6.343*	-8.459*	-6.308*	-1.568	-6.935*	–

Table S2. Performance comparison of Cases 3, 2, and 4 during the validation period, with runoff generation parameters held constant as in Case 4. Performance is quantified by the KGE metrics, with the best value for each sub-basin shown in bold.

	Hanzhong	Yangxian	Youshui	Lianghekou	Shiquan
Case 3	0.494	0.632	0.376	0.589	0.672
Case 2	0.492	0.630	0.372	0.582	0.670
Case 4	**0.521**	**0.637**	**0.446**	**0.730**	**0.689**

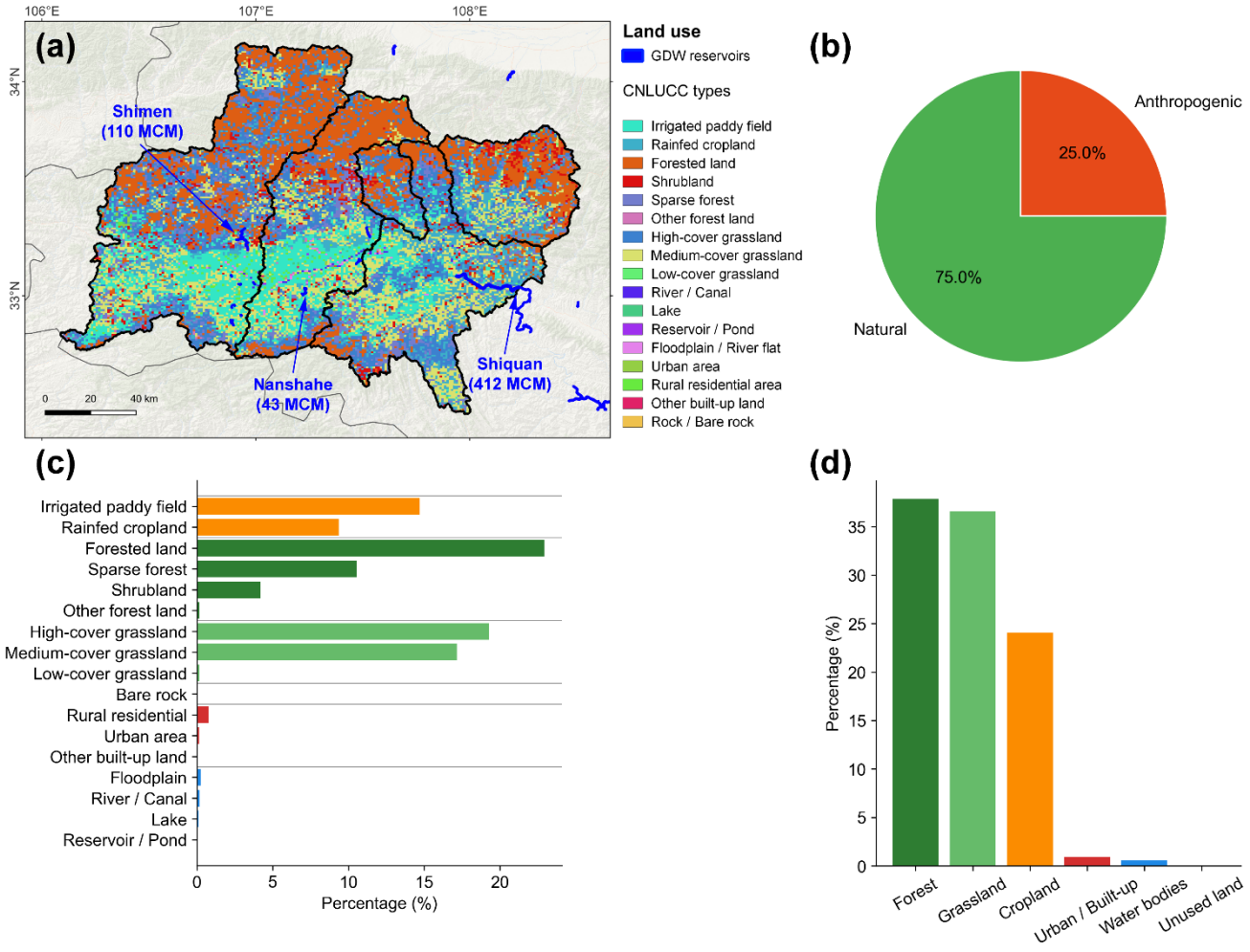

Figure S1. Land use analysis of the Upper Han River Basin based on the CNLUCC (Xu et al., 2018) and GDW (Lehner et al., 2024) datasets. (a) Spatial distribution of land use, with the three major dams (Shimen, Nanshahe, and Shiquan) highlighted in azure and having maximum storage capacities of 110, 43, and 412 MCM (million cubic meters), respectively. (b) Proportions of anthropogenic versus natural land use, where cropland and urban & built-up areas (based on the primary land use classification) are considered anthropogenic. (c) Secondary land use composition. (d) Primary land use composition.

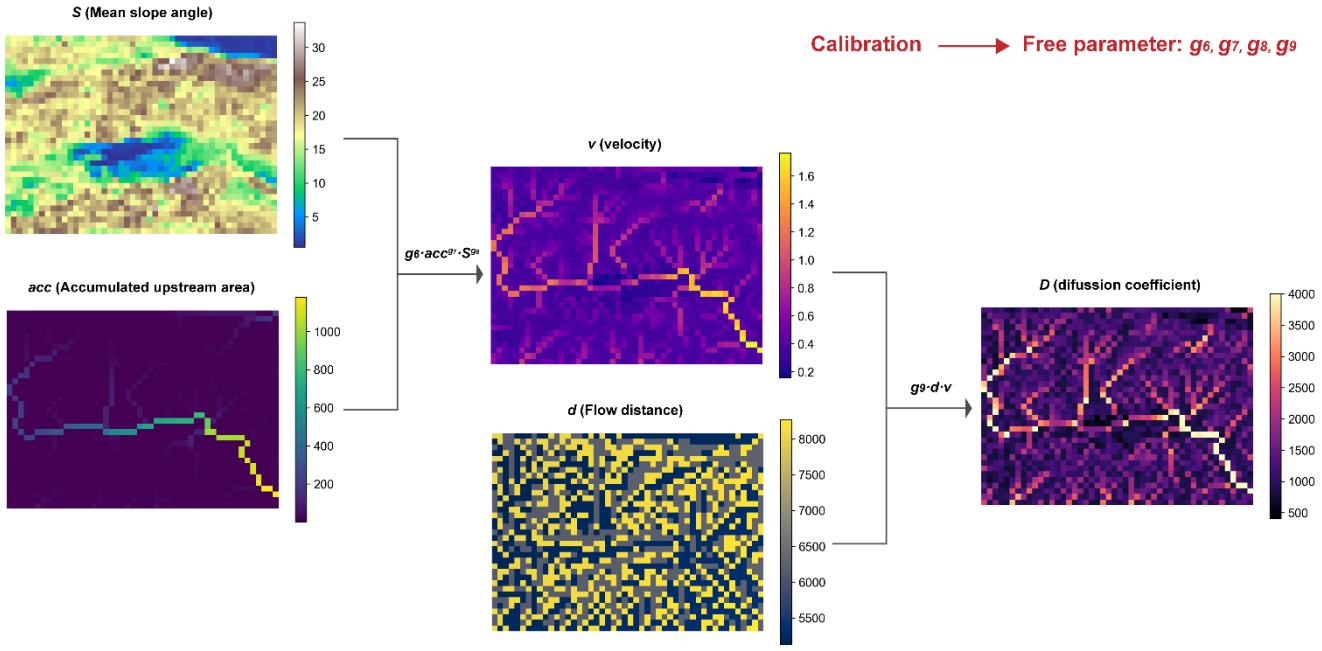

30 **Figure S2. Refinement of the MPR-based regionalization of RVIC parameters. Spatially distributed velocity and diffusion coefficients are estimated using transfer functions (Table 2) driven by topographic attributes and calibratable g-parameters.**

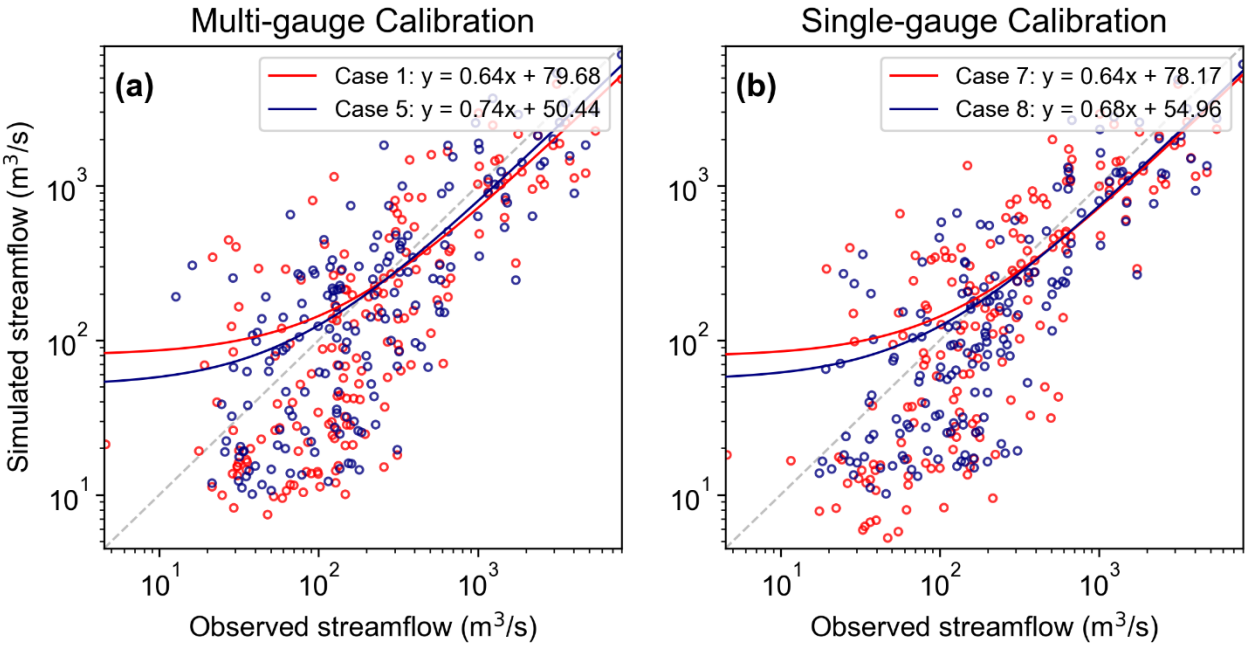

Figure S3. Scatterplots with least-squares regression lines comparing observed and simulated daily streamflow at the Shiquan station during the validation period, under different case configurations. The grey dashed line represents the 1:1 line. Flows below 1000 $m^3 s^{-1}$ were randomly thinned for clarity, and both axes are shown on a logarithmic scale.

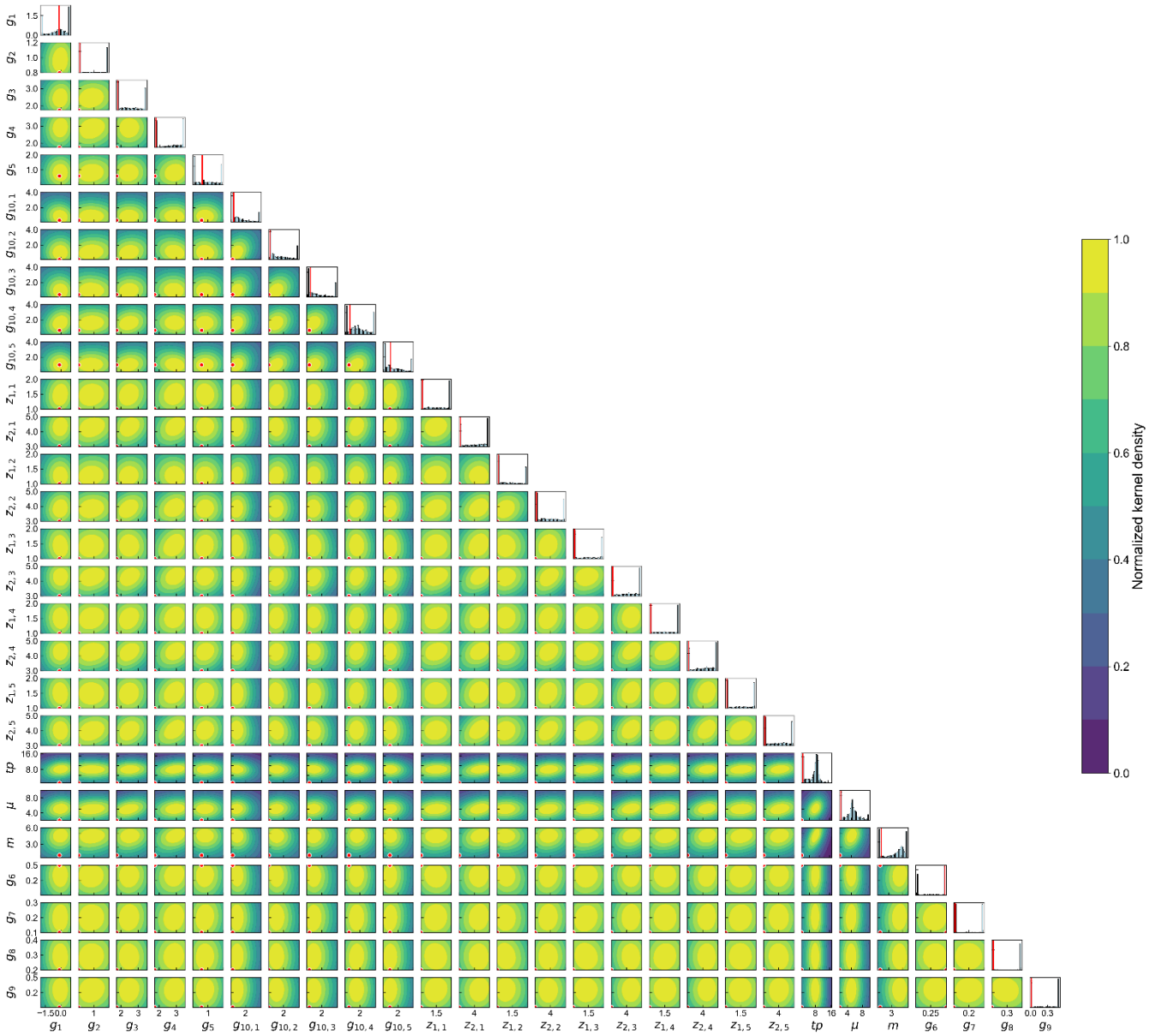

Figure S4. Post-calibration parameter distributions for Case 8. The optimal parameters are shown as red dots and lines. The background contours represent the standardized kernel density estimate derived from all candidate solutions, where yellow shading corresponds to high probability density regions. The histograms along the diagonal represent the marginal distribution of each individual parameter.

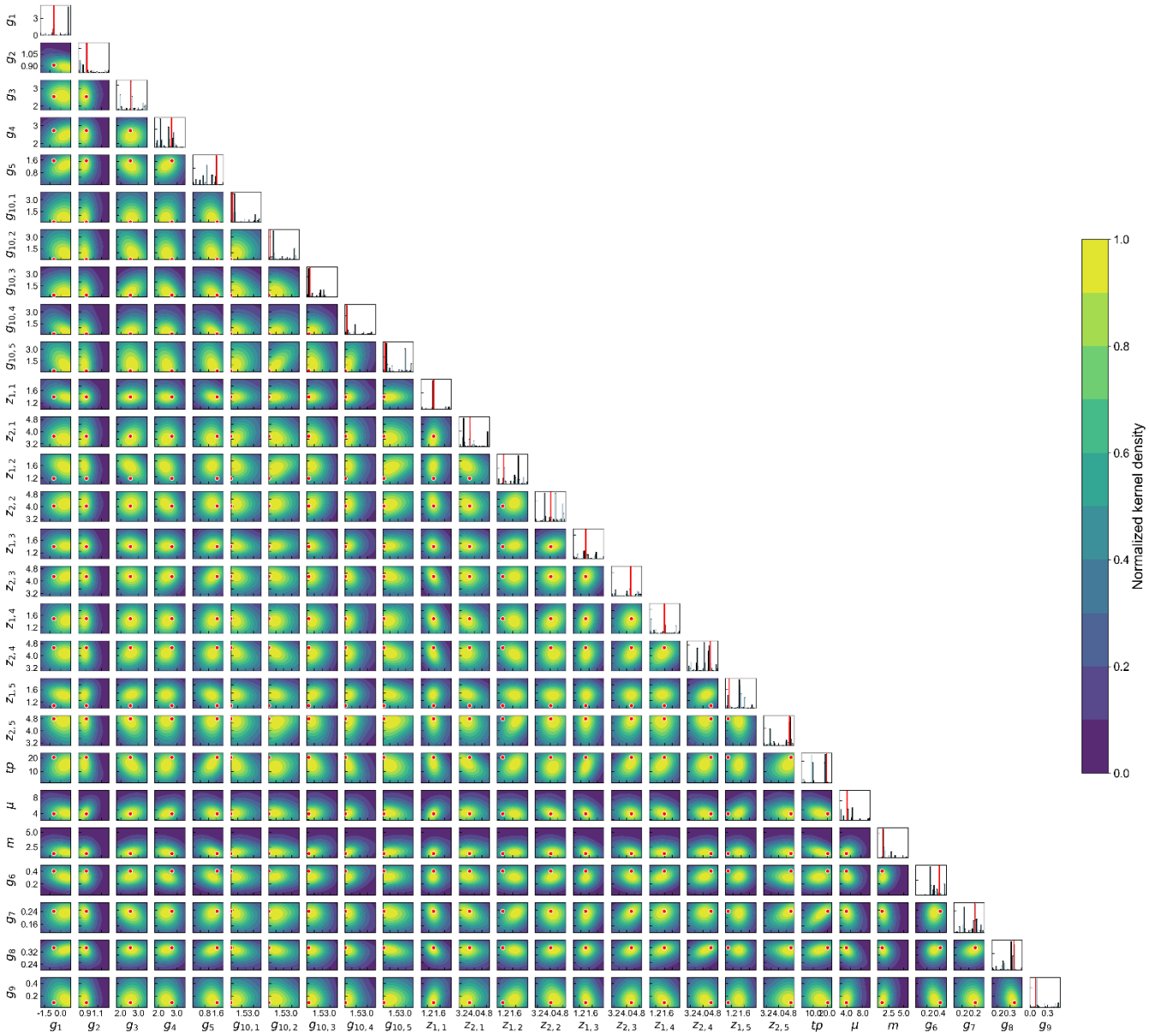

Figure S5. Post-calibration parameter distributions for Case 5, following the same visualization conventions as Fig. S4. While the overall structure is similar, Case 5 exhibits more concentrated posterior distributions and different optimal values.

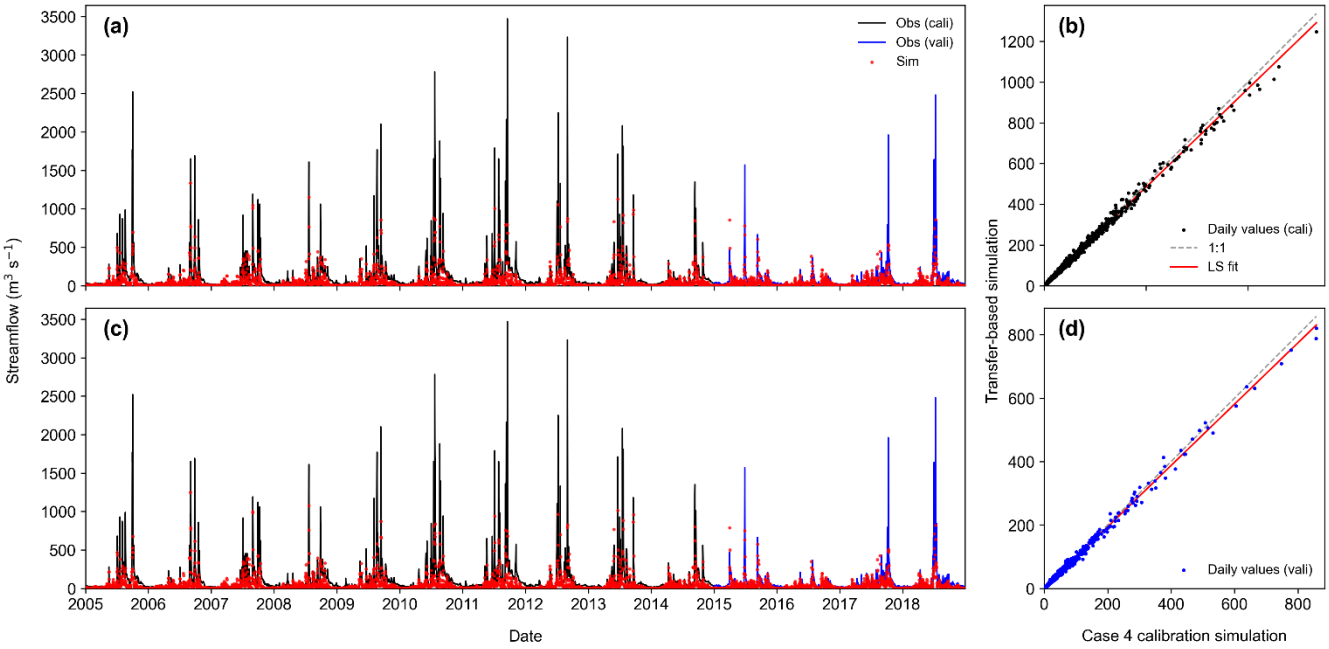

45 **Figure S6. Leave-one-out evaluation of parameter transferability for the Hanzhong sub-basin. Panels (a) and (c) display the simulated daily hydrographs for the baseline Case 4 calibration and the transfer-based simulation, respectively. Panels (b) and (d) present the corresponding scatter plots comparing the Case 4 baseline and transfer-based simulation for the calibration and validation periods.**

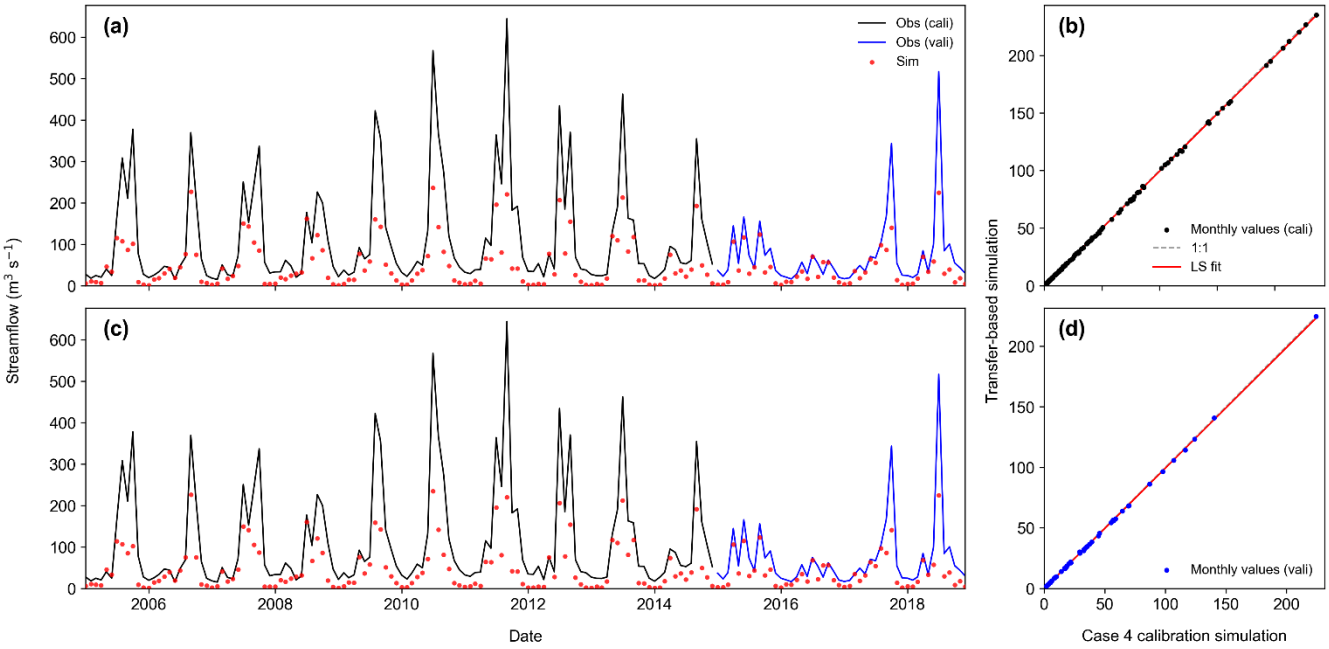

Figure S7. Leave-one-out evaluation of parameter transferability for the Hanzhong sub-basin, following the same visualization conventions as Fig. S6 but at a monthly timescale.

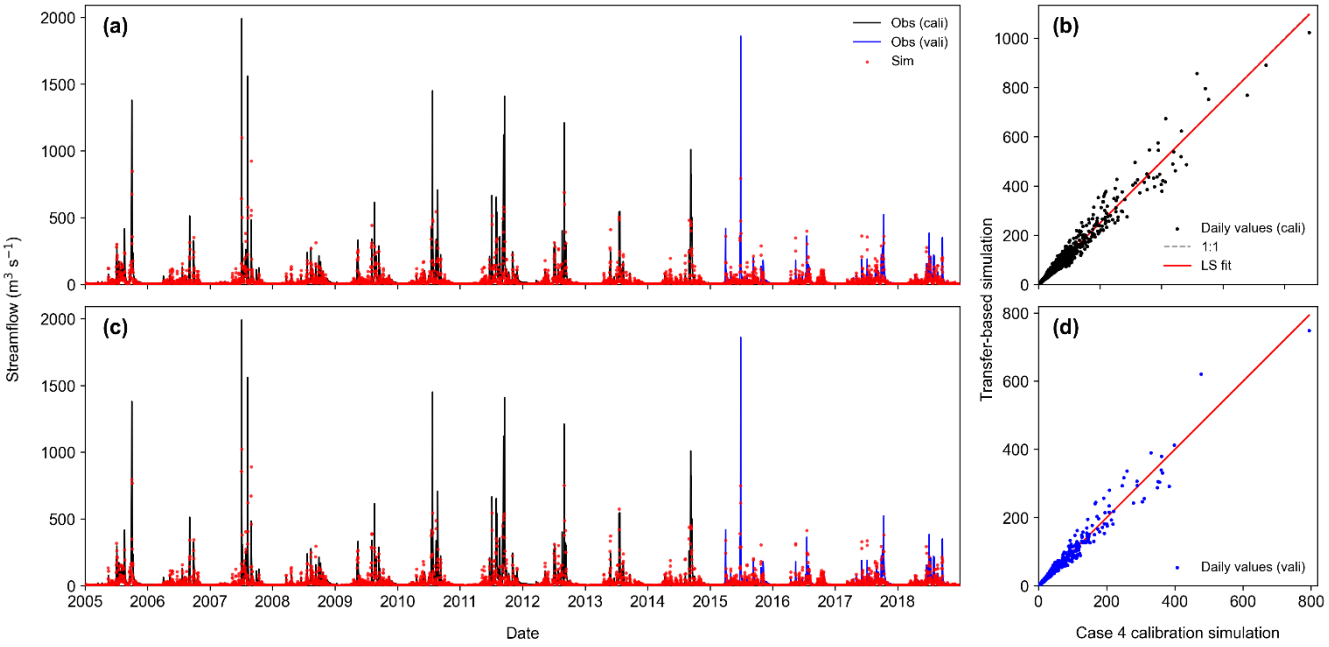

Figure S8. Leave-one-out evaluation of parameter transferability for the Lianghekou sub-basin, following the same visualization conventions as Fig. S6.

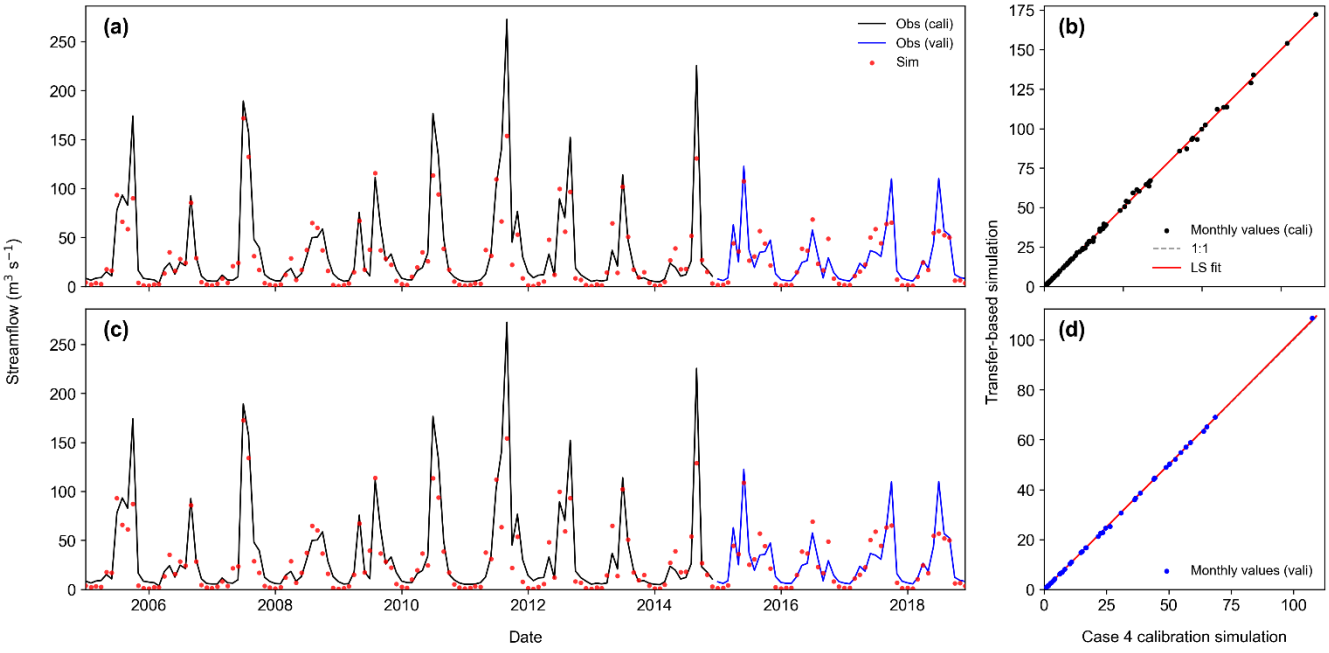

Figure S9. Leave-one-out evaluation of parameter transferability for the Lianghekou sub-basin, following the same visualization conventions as Fig. S6 but at a monthly timescale.

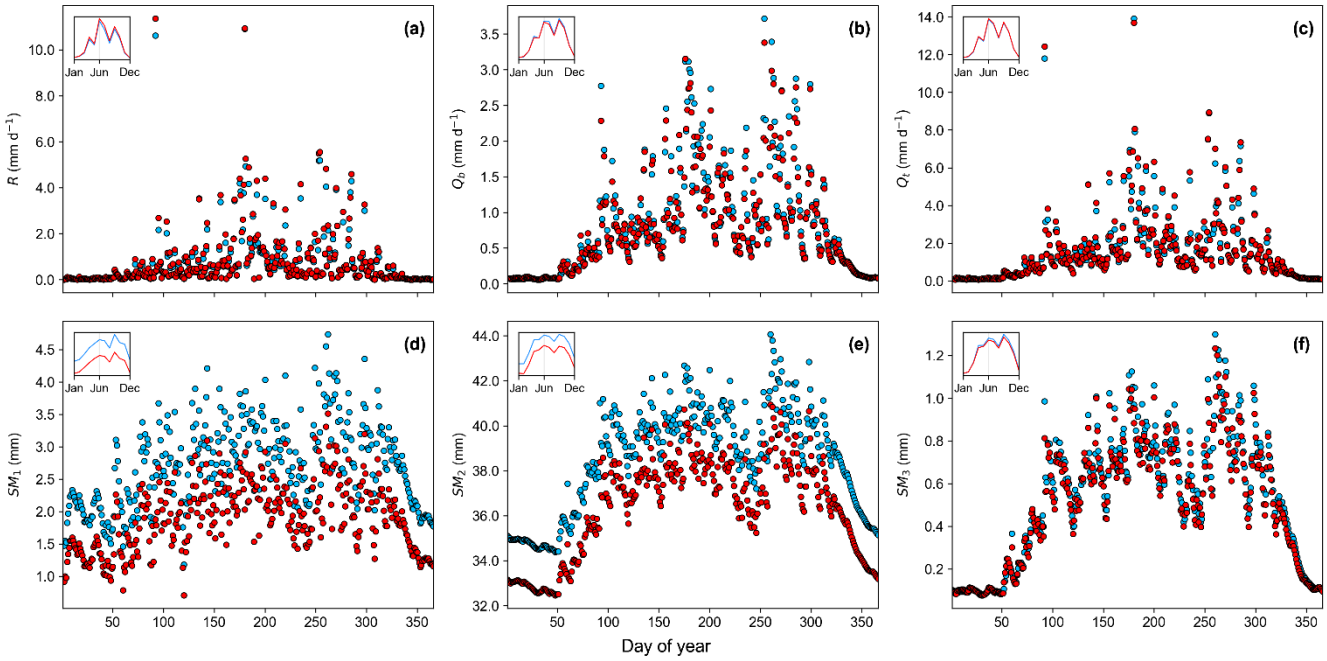

Figure S10. Long-term daily climatology of simulated hydrological variables for Case 4 (blue) and Case 5 (red). The primary variables are: (a) surface runoff (R), (b) baseflow (Q_b), (c) total runoff (Q_t), and (d–f) soil moisture in the top, middle, and bottom layers (SM_1, SM_2, SM_3), respectively. Insets in the upper-left corners show the corresponding mean monthly climatology for each variable.

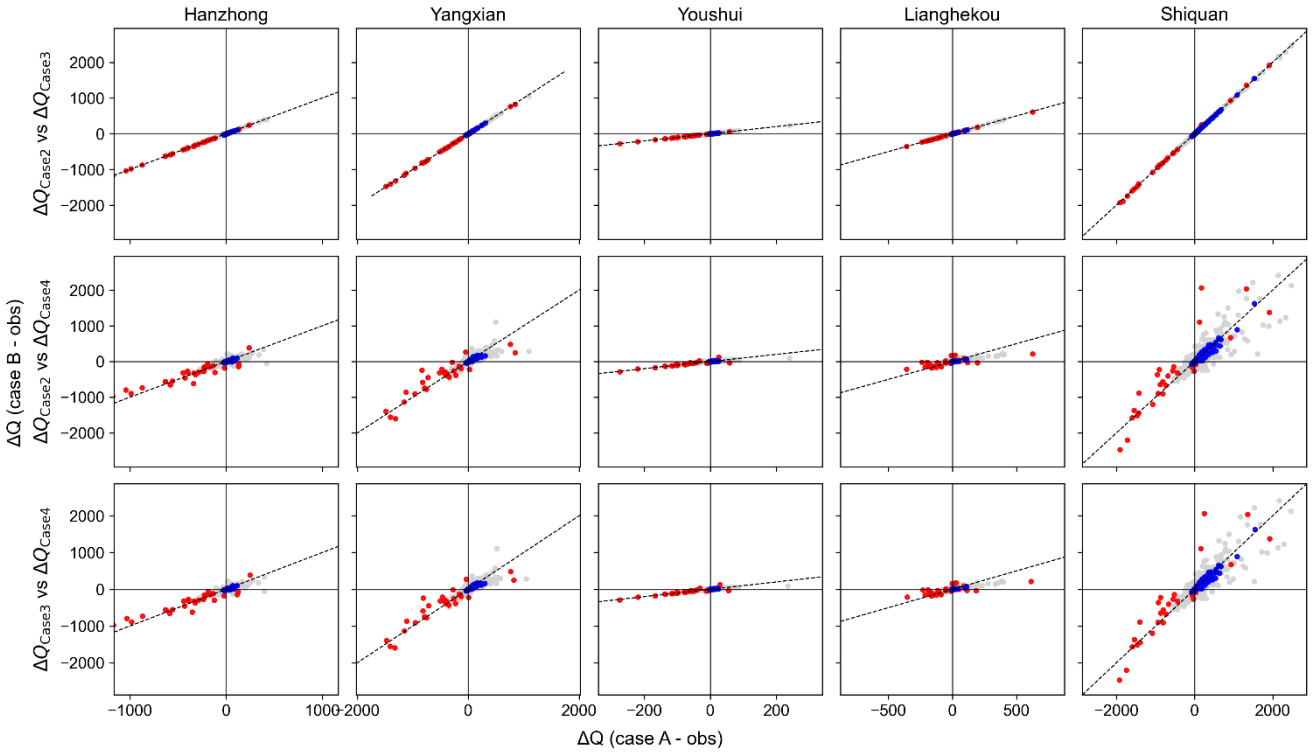

Figure S11. Scatter plots of simulated residuals (Δ*Q*) for Cases 3, 2, and 4 during the validation period, using the runoff generation parameters from Case 4. Red and blue dots represent high flows (exceedance probability < 2%) and low flows (exceedance probability > 70%), respectively. The dashed line indicates the 1:1 line.